New Heating Characteristics of a Radio Frequency Rectangular Resonant Cavity Applicator Using Various Antennas for Hyperthermic Treatment

Yutaka Tange [1], Yasushi Kanai [2], Yoshiaki Saitoh [3], and Tatsuya Kashiwa [4]

[1] Graduate School of Science and Technology
Niigata University, Niigata, 950-2181, Japan

[2] Department of Information and Electronics Engineering
Niigata Institute of Technology, Kashiwazaki, 945-1195, Japan

[3] Department of Biocybernetics, Faculty of Engineering
Niigata University, Niigata, 950-2181, Japan

[4] Department of Electrical and Electronic Engineering
Kitami Institute of Technology, Kitami, 090-8507, Japan

Abstract **–** The heating characteristics of a radio frequency rectangular resonant cavity applicator excited by various antennas are investigated for use in hyperthermic treatment. The coupled electromagnetic and heat-transfer equations are solved to obtain the heating characteristics. Two types of antennas and three types of dielectric phantoms are used in the calculations and measurements. Clear differences in the heating characteristics are observed for these phantoms and antennas. Previously, we were only able to heat up the surface or end regions of the phantom, while it is now possible to uniformly heat up the deeper regions with the current applicator. Therefore, this applicator is suitable for hyperthermic treatment.

Keywords **–** Cavity resonators, dielectric phantom, FDTD methods, finite element methods, and hyperthermia.

I. INTRODUCTION

World Health Organization (WHO) statistics suggest that six million humans in the world die of cancer and ten million new patients are added every year [1].

Hyperthermia is a cancer treatment which exposes human tissues to high temperatures in order to irreparably damage or kill cancer cells. The treatment focuses on the difference in heat sensitivity between nomal (alive until $44\,^{\circ}C$) and cancer cells (dead above $42.5\,^{\circ}C$) [2]. In this method, the region around the tumor including healthy tissue is heated by, for example, electromagnetic energy. By comparison with a surgical cure, radiation therapy, and anticancer drug therapy, hyperthermia has the possibility of decreasing cancer patients' pain and suffering.

Many heating applicators for hyperthermia have been developed. For example, radio frequency heating [3] and microwave heating [4] applicators have been used for clinical treatment. However, these heating methods have several problems since the heating region is limited to areas near the surface of the body and moreover there are the effects of blood flow and complex human organs. Annular phased array (APA) systems, using the principle of phased arrays [5], [6], can heat deep-seated tumors selectively. However, it is difficult to control the phases and the amplitudes of multiple antennas in order to focus the electromagnetic energy [7], [8].

We have previously reported the analysis of, and experiments on, a reentrant resonant cavity applicator for hyperthermic treatment [9]-[11]. The applicator was able to heat a deep-seated region of a disk-shaped dielectric phantom, but a torso-shaped dielectric phantom similar in length to a human body could not be heated. Therefore, we developed a rectangular resonant cavity applicator using two antennas to realize heating of a deep region for a torso-shaped dielectric phantom. In our previous papers, the antennas were not modeled but the magnetic energy was supplied at a single point [12], [13]. Therefore, it is possilbe to obtain more accurate solutions if the antennas are modeled more precisely. In addition, we had no proper phantom with regard to electrical properties, especially electrical conductivity leading to poor experimental results. Note that we had already considered the various organs and metabolism including blood flow, and found that the

most critical issue is the design of the heating system, in particular, how the electromagnetic energy is directed towards the targeted region [11].

In this paper, we describe the analysis and the experiments of the heating technique for a deep-seated region in an RF rectangular resonant cavity applicator. In the experiments, we prepared TX-151 (a commercial powder for dielectric phantom fabrication designed with electrical and thermal constants close to muscle), clay, and the original phantoms and measured the frequency and temperature dependencies of the electrical constants. Then, dipole and L-type antennas were constructed and placed inside the applicator. First, two kinds of phantoms (TX-151 and clay phantoms) were used because we wanted to investigate how electrical constants affect the heating patterns. Next, we applied the original phantoms that have electrical constants close to that of human muscle by adjusting the initial temperature. It is possible to heat the center of the phantom if the antenna is moved appropriately. In addition, we had already found that the applicator fed by two antennas was better at heating the deeper region [13]. Therefore, we moved the antennas away from the applicator's center. In the analyses, the coupled electromagnetic and heat-transfer equations are solved to obtain the heating characteristics by using the FD-TD method [14] and FEM [10], [11], [13]. The antennas were modeled exactly. The experiments demonstrate the validity of the electromagnetic-heat transfer calculations and the possibility of heating deep-seated tumors.

II. RF HYPERTHERMIC SYSTEM AND RESONANT CAVITY APPLICATOR

As shown in Fig. 1, the system consisted of a signal generator (Tokyo HY-Power Labs., Inc. G1057VG), a set of high frequency electric power amplifiers (Niigata Tsushinki Co., Ltd., PA2000J), two power meters (BIRD Electronic Corp., Model 43), three custom impedance matching boxes, a set of dipole antennas or a set of L-type antennas, a custom balloon [15] with a coaxial line (Kyowa Ltd., 10D2V) used for dividing the RF power into two parts of the antenna, and a resonant cavity applicator. One L-type antenna, one matching box, and the balun are removed to make a single L-type antenna system.

The arrangement of the setup is shown in Fig. 2. The resonant cavity applicator is formed from 0.5 mm thick copper with dimensions 1300 mm × 1450 mm × 1500 mm. The wooden table consisted of a top plate with dimensions 1200 mm × 35 mm × 400 mm and four legs 70 mm in diameter and 555 mm in length. The dielectric phantom was placed on the table. The dipole antennas were placed beside the phantom at the center of the applicator in the x-direction. We were able to heat the distal parts (surface or end regions) of the phantom [13] and it was possible to heat the center of the phantom if the antennas were displaced appropriately [16]. Therefore, we placed the antenna 450 mm from the center with regard to the x-axis, as shown in Fig. 3. In addition, we had already found that the applicator fed by two antennas was better able to heat the deeper region [13]. We placed the antennas 450 mm and – 450 mm from the center with respect to the x-axis, as shown in Fig. 4. A dielectric phantom was used for the experiments to heat the deeper region before considering the clinical stage. The resonant state and the heating process for the rectangular cavity are discussed in the next section.

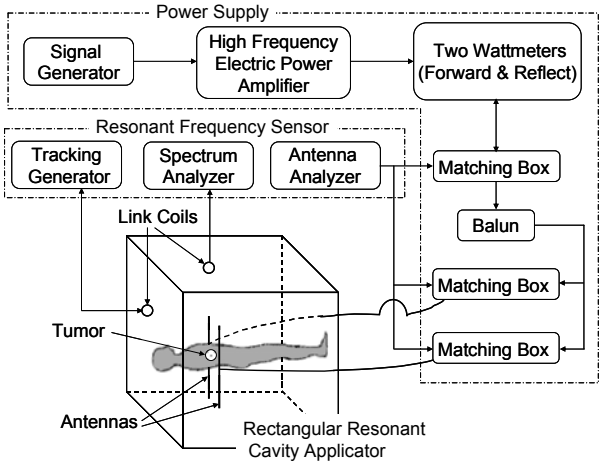

Fig. 1. Hyperthermic system schematic drawing.

III. VARIOUS DIELECTRIC PHANTOMS

We prepared three types of static dielectric phantoms: a TX-151 dielectric phantom 280 mm in diameter and 1200 mm in length, a clay phantom 300 mm in diameter and 1000 mm in length and an original dielectric phantom 280 mm in diameter and 1200 mm in length. The original dielectric phantom was composed of TX-151 solidifying powder (12.8 %) (Oil Center Research, Inc.), water (85.7 %) and additional agar powder (1.5 %) (Junsei Chemical Co., Ltd.). As compared to the TX-151 phantom, this original phantom has electrical properties similar to human muscle for a wide temperature range. As shown in Fig. 5, the temperature dependences of the electrical properties for these phantoms were measured using our measurement system prior to the calculations [17]. The electrical conductivity σ and the relative permittivity ε_r of human muscle in the RF range are approximately 0.7

S/m and 70, respectively [18]. Therefore, proper electrical constants are obtainable when the original dielectric phantom temperature is approximately $20\,°C$. Before the experiments, we kept both the room temperature and the dielectric phantom's temperature at approximately $20\,°C$ for more than 12 hours by using an air conditioner. The properties were measured at the resonant frequencies (50 MHz, 60 MHz, and 85 MHz) in the cavity as shown in section 2. The thermal properties of these phantoms are shown in Table 1 [10], [19]. The electrical properties of the wooden table, only used for electromagnetic field analysis were assumed to be $\varepsilon_r = 1.88$ and $\sigma = 0.0003$ S/m [20].

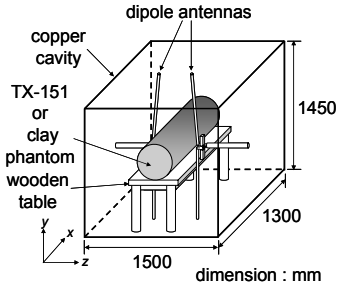

(a) A set of dipole antennas.

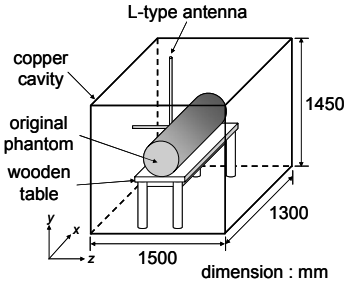

(b) L-type antenna.

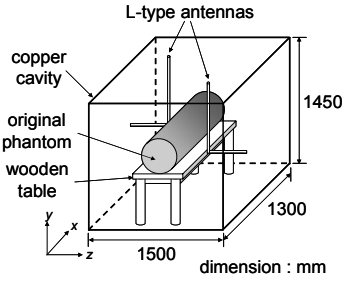

(c) A set of L-type antennas.

Fig. 2. Arrangement of a rectangular resonant cavity applicator, a phantom, an antenna(s), on the wooden table.

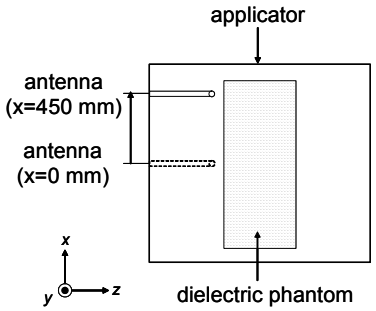

Fig. 3. Two locations of the L-type antenna (x = 0 mm and 450 mm): x = 450 mm from the center with respect to the x-axis was found to be appropriate.

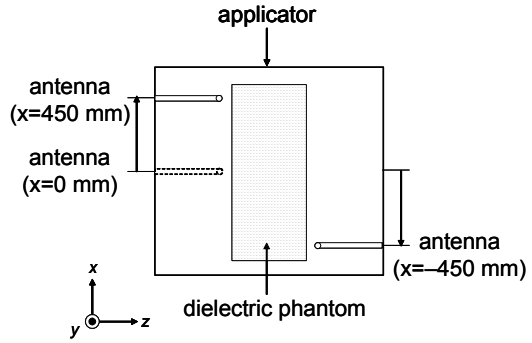

Fig. 4. Two locations for the L-type antennas (x = 450 mm and – 450 mm).

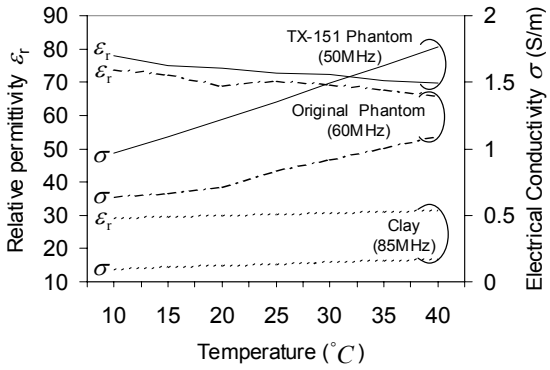

Fig. 5. Measured relative permittivity and electrical conductivity of the three phantoms.

IV. CALCULATION METHOD

The flow diagrams of the electromagnetic field calculations and heat-transfer calculations are shown in Fig. 6. We have modeled the cavity containing the dielectric phantom, the antenna(s), and the wooden table for the electromagnetic calculations. Note that the cavity walls were assumed to be perfect electrical

conductors.

We have used the three-dimensional finite-difference time-domain (FDTD) method [14] to solve Maxwell's equations:

$$\nabla \times \mathbf{E} = -\mu \frac{\partial \mathbf{H}}{\partial \mathrm{t}}, \tag{1}$$

$$\nabla \times \mathbf{H} = \sigma \mathbf{E} + \varepsilon \frac{\partial \mathbf{E}}{\partial \mathrm{t}} \tag{2}$$

where, μ, σ, and ε are respectively permeability, electrical conductivity, and permittivity. A current excitation source with a load impedance of 50 Ω at the gap was assumed for the dipole antennas. A voltage source with a pure sinusoidal wave was applied to the L-type antenna. Thin wire approximation [21] was used to model the dipole and L-type antennas. The whole volume of the cavity applicator was divided by our automatic mesh generator [22] into regular cells with a side length of 25 mm, as shown in Fig. 7.

After analyzing the electromagnetic field distributions, the electromagnetic energy applied to the phantom was evaluated as,

$$\dot{\mathrm{Q}} = \frac{1}{\mathrm{T}} \sigma \int |\mathbf{E}|^2 \, \mathrm{dt} \, . \tag{3}$$

The output data $\dot{\mathrm{Q}}$ were interpolated at regular intervals of 12.5 mm.

The heat-transfer equations

$$\rho c \frac{\partial \mathrm{T}}{\partial \mathrm{t}} = \lambda \nabla^2 \mathrm{T} + \dot{\mathrm{Q}}, \tag{4}$$

$$\mathrm{q} = \alpha_{\mathrm{c}} \left(\mathrm{T} - \mathrm{T}_{\mathrm{c}} \right) \tag{5}$$

are solved using three dimensional FEM because it is easier to set boundary conditions for FEM than for FDM. ρ, c, λ, q, α_{c}, and T_{c} denote respectively volume density of mass, specific heat capacity, thermal conductivity, heat flux, heat transfer coefficient, and the external temperature. The thermal constants of the TX-151 and original phantom were assumed to be as shown in Table 1 as both phantoms consisted of mostly water. In the heat-transfer calculations, only the phantom was modeled as it was discovered that the wooden table did not affect the temperature distributions. Brick elements 12.5 mm on each side were used, as shown in Fig. 8, such that the calculated electromagnetic energy from the FDTD calculation could be transferred precisely. That is, the average value of the eight-point nodal data obtained by FDTD analysis is considered to be the data of one element for FEM analysis.

Table 1. Thermal constants of dielectric and clay phantom.

TX-151 or Original Phantom	Volume density of mass	1030 (kg/m³)
	Specific heat capacity	3150 (J/kg°C)
	Thermal conductivity	0.555 (W/m°C)
	Heat transfer coefficient	5 (W/m²°C)
	Relative permeability	1
Clay Phantom	Volume density of mass	1700 (kg/m³)
	Specific heat capacity	1800 (J/kg°C)
	Thermal conductivity	1.2 (W/m°C)
	Heat transfer coefficient	5 (W/m²°C)
	Relative permeability	1

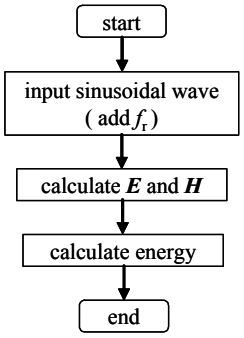

(a) Electromagnetic field analysis.

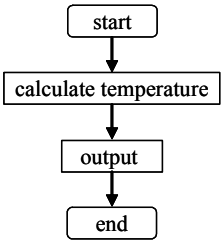

(b) Heat-transfer analysis.

Fig. 6. Flow diagrams of electromagnetic field and heat-transfer analysis.

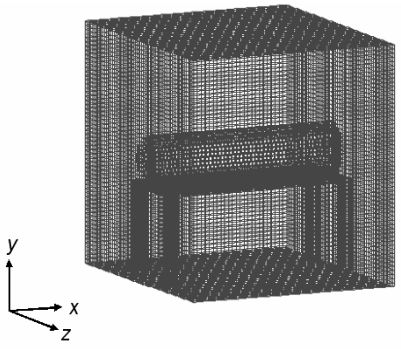

Fig. 7. FDTD mesh used for electromagnetic field analyses, where a resonant cavity applicator, dielectric phantom, a wooden table, and L-type antennas are modeled.

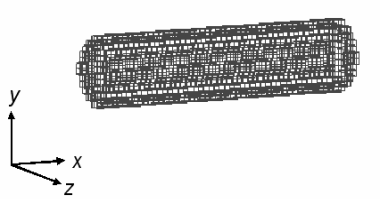

Fig. 8. FEM mesh used for heat-transfer analyses. Only the dielectric phantom is modeled.

V. EXPERIMENTAL PROCEDURE

Electromagnetic energy of 400 watts in the frequency range of 50 MHz – 85 MHz at the amplifiers' terminal was generated from the amplifiers. While the phantom is heated, the reflected power increases because of the temperature dependencies of the material properties. The amount of reflected power is minimized by adjusting the matching box during the heating process, i.e. the resonant state is maintained by changing the capacitance of the matching box. After a heating process of 30 minutes, the phantom was cut, and the temperature distribution was observed using a thermograph (Fujitsu Infra-Eye210).

VI. RESULTS AND DISCUSSION

A. Validity of Calculation

In electromagnetic analysis using finite-difference time-domain methods, a stable condition exists if the following relationship is valid [23],

$$\text{mesh size} \leq \lambda_{\text{wavelength}} / 10 \qquad (6)$$

where $\lambda_{\text{wavelength}}$ is the wavelength inside the dielectric phantom. A mesh size of 25 mm in our calculation is sufficient to satisfy this condition as a minimum value to achieve a stable condition in this case is 60 mm.

B. Comparison of Measured and Calculated Results

The measured and calculated results obtained in this study are shown in Figs. 9 and 10 for TX-151 and clay phantoms. The experimental conditions, starting temperature T_0 of the phantoms, surrounding temperature T_c, and resonant frequency f_r, are shown in the figure captions.

Whereas the tendencies of the measured temperature distributions for the TX-151 phantom and the original phantom agree with the calculated ones, the result for the clay phantom varies from the calculated one.

The major reasons for this discrepancy in temperature distributions are most likely caused by the differences in thermal properties of the clay phantom and deformation of the TX-151 and original phantoms between the experiments and calculations. It is also seen, from Fig. 10 (a), that the deep region of the phantom exhibiting low electrical conductivity can be heated up easily as we have noted previously [10].

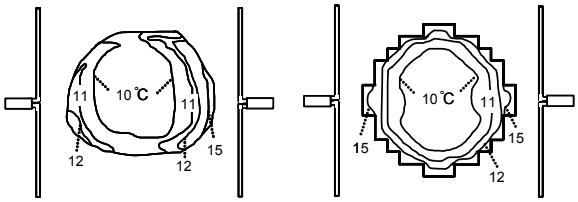

(a) Measured result (f_r = 51.37MHz – 51.45 MHz)

(b) Calculated result (f_r = 51.37 MHz)

Fig. 9. Measured and calculated temperature distributions of the center of the cross section in the dielectric phantom fed by two antennas with opposite phase, where initial temperature of the phantom T_0 and external temperature T_c were $10\,°C$ and $15\,°C$, respectively.

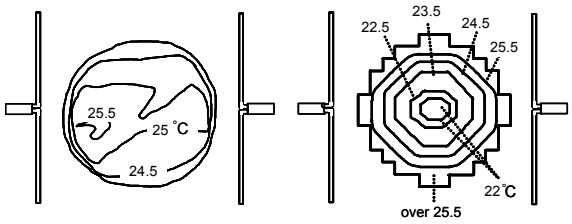

(a) Measured result (f_r = 84.80 MHz)

(b) Calculated result (f_r = 84.80 MHz)

Fig. 10. Measured and calculated temperature distributions of the center of the cross section in the clay phantom fed by two antennas with opposite phase, where T_0 and T_c of the clay were $21.8\,°C$ and $23.5\,°C$, respectively.

Measured and calculated temperatures are compared in Figs. 11 through 13 for an original phantom where the antenna was located at x = 0 mm in Fig. 11 and at x = 450 mm in Figs. 12 and 13. Note that the electrical conductivity and the relative permittivity of human muscle in the RF range are approximately 0.7 S/m and 70, respectively [18]. Therefore, the starting temperatures were set such that the phantoms' electrical conductivities were closer to that of human muscle. The increases in temperature of the deep region from the original state in Figs. 11 and 12 were $0.2\,°C$ and $1.9\,°C$, respectively. Therefore, it is very important to move the L-type antenna away from the applicator's center to achieve heating of the deep region. Comparing

Figs. 12 and 13 reveals that a small difference in starting temperature greatly alters the heating pattern, that is, the heating properties are sensitive to the initial electrical constants.

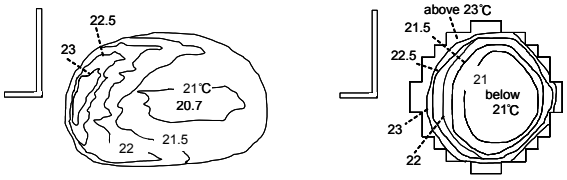

(a) Measured result (f_r = 61.62 MHz)

(b) Calculated result (f_r = 61.62 MHz)

Fig. 11. An L-type antenna (solid line) was placed at x = 0 mm. Calculated and measured temperature distributions on a cross section at x = 0 mm, where T_0 and T_c were 20.5 °C and 20.8 °C, respectively.

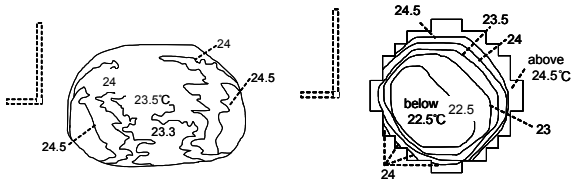

(a) Measured result (f_r = 62.23 MHz – 62.27 MHz)

(b) Calculated result (f_r = 62.27 MHz)

Fig. 12. An L-type antenna (dotted line) was placed at x = 450 mm. Calculated and measured temperature distributions on a cross section at x = 0 mm, where, T_0 and T_c were 21.4 °C and 21.5 °C, respectively.

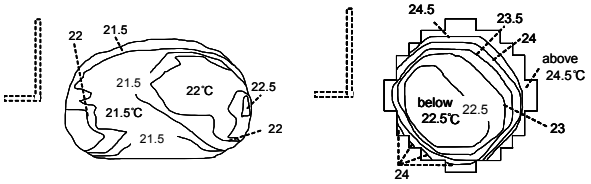

(a) Measured result (f_r = 62.20 MHz)

(b) Calculated result (f_r = 62.20 MHz)

Fig. 13. An L-type antenna (dotted line) was placed at x = 450 mm. Calculated and measured temperature distributions on a cross section at x = 0 mm, where T_0 and T_c were 19.6 °C and 19.9 °C, respectively.

The measured and calculated results fed by two antennas with the same and opposite phases of voltage distribution are shown respectively in Figs. 14 and 15 for the original phantom. Note that opposite phase implies that the two energies with a phase difference of 180^o are applied to two antennas. The increases in temperature of the deeper region from the original state in Figs. 14 and 15 were 1.9 °C and 1.8 °C, respectively. Comparison of the results of the single antenna and a set of L-type antennas with the same and opposite phases showed that the applicator, fed by two antennas with the same phase, heated the deeper region more uniformly. These results indicate that better heating patterns were obtained than in the previous results [9] - [13].

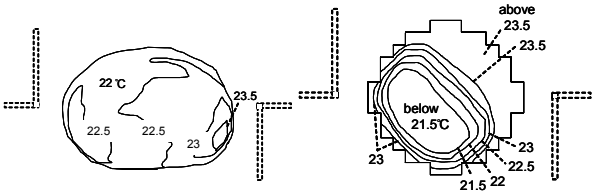

(a) Measured result (f_r = 62.82 MHz)

(b) Calculated result (f_r = 62.82 MHz)

Fig. 14. A set of L-type antennas (dotted line) fed by the same phase of voltage distribution were placed at x = 450 mm and x = – 450 mm. Calculated and measured temperature distributions on a cross section at x = 0 mm, where T_0 and T_c were 20.1 °C and 20.4 °C, respectively.

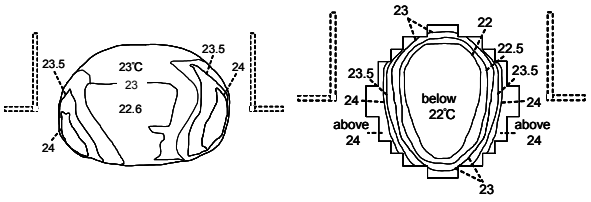

(a) Measured result (f_r = 61.81 MHz)

(b) Calculated result (f_r = 61.81 MHz)

Fig. 15. A set of L-type antennas (dotted line) fed by the opposite phase of voltage distribution were placed at x = 450 mm and x = – 450 mm. Calculated and measured temperature distributions on a cross section at x = 0 mm, where T_0 and T_c were 20.3 °C and 21.3 °C, respectively.

The measured and calculated results shown here are only for the cross section located at x = 0 mm, and note that the other cross sections as well as the central cross section (x = 0 mm) were also heated. If the temperature of the external parts of the dielectric phantom is higher than the internal parts, then the cooling method using pure water can be applied [10], [11].

In the future, calculations considering the organs and blood flow are necessary with finer FD-TD cells as well as measurements to obtain a better heating pattern that is capable of treating deep-seated cancer tumors.

VII. CONCLUSION

The heating characteristics of an RF hyperthermia applicator for deep-seated regions have been investigated using both calculated and experimental results. We have also prepared various dielectric phantoms. The initial temperature was adjusted so that the torso-shaped phantoms used for the experiments had electric characteristics similar to that of human muscle. We have constructed dipole and L-type antennas and placed them at appropriate positions in a rectangular resonant cavity applicator.

Better heating patterns, exhibited by uniformly heating a deeper region can be obtained by moving the antenna away from the applicator's center. In addition, it was found that the applicator, fed by a set of L-type antennas with the same phase, heated the deeper region more uniformly. Better heating patterns with regard to heating in a deep-seated region were obtained when compared to our previous work.

In the future, calculations considering the organs and blood flow are necessary as well as measurements to obtain a better heating pattern that treats deep-seated cancer tumors before the clinical stage can be undertaken.

ACKNOWLEDGMENT

The authors would like to acknowledge Messrs Hiroki Ishiwatari, Tsuyoshi Satoh, and Hiroaki Shimazaki of our laboratory in Niigata University for their experimental and related assistance and Mr. Tsukasa Shiga of Niigata Institute of Technology for supplying the calculated results.

REFERENCES

[1] World Health Organization web site [Online]. Available : (http://www.who.int/cancer/en/).

[2] W. C. Dewey, and L. E. Hopwood, "Cellular responses to combinations of hyperthermia and radiation," *Radiology*, vol. 123, pp. 463-474, 1977.

[3] H. Takahashi, R. Tanaka, M. Watanabe, K. Kakinuma, T. Suda, S. Takahashi, H. Masuda, A. Saito, and T. Nakajima, "Clinical results of RF interstitial hyperthermia for malignant brain tumors," *Japanese Journal of Hyperthermic Oncology*, vol. 11, no. 1, pp.61-67, March 1995 (in Japanese).

[4] C. H. Durney, and D. A. Christensen, *Introduction to Bioelectromagnetics*, Boca Raton: CRC, pp. 151-153, 1999.

[5] P. F. Turner, "Regional hyperthermia with an annular phased array," *IEEE Trans. on Biomed. Eng.*, vol. 31, no. 1, pp. 106-114, Jan. 1984.

[6] N. Terada and Y. Amemiya, "The performance of the dipole array applicator for radiofrequency hyperthermia," *The IEICE Transactions on Communications*, vol. J67-B, no. 2, pp. 163-170, Feb. 1984 (in Japanese).

[7] N. Siauve, L. Nicolas, C. Vollaire, A. Nicolas, and J. A. Vasconcelos, "Optimization of 3-D SAR distribution in local RF hyperthermia," *IEEE Trans. on Magn*., vol. 40, no. 2, pp. 1264-1267, Mar. 2004.

[8] P. Wust, B. Hildebrandt, G. Sreenivasa, B. Rau, J.Gellermann, H. Riess, R. Felix, and P. M. Schlag, "Hyperthermia in combined treatment of cancer," *The LANCET Oncology*, vol. 3, pp. 487-497, Aug. 2002.

[9] K. Kato, J. Matsuda, and Y. Saitoh, "A re-entrant type resonant cavity applicator for deep-seated hyperthermia treatment," *Proc*. *Annual Int'l Conf. of the IEEE Eng. in Medicine and Biology Society*, vol. 11, pp. 1712-1713, Nov. 1989.

[10] Y. Kanai, T. Tsukamoto, K. Toyama, Y. Saitoh, M. Miyakawa, and T. Kashiwa, " Analysis of a hyperthermic treatment in a reentrant resonant cavity applicator by solving time-dependent electromagnetic- heat transfer equations," *IEEE Trans. on Magn*., vol. 32, no. 3, pp. 1661-1664, May 1996.

[11] Y. Kanai, T. Tsukamoto, Y. Saitoh, M. Miyakawa, and T. Kashiwa, "Analysis of a hyperthermic treatment using a reentrant resonant cavity applicator for a heterogeneous model with blood flow," *IEEE Trans. on Magn*., vol. 33, no. 2, pp. 2175-2178, Mar. 1997.

[12] S. Soeta, S. Yokoo, M. Shimada, Y. Kanai, and J. Hori, "Eigenmode analysis of a parallelepiped resonator for hyperthermic treatment by using FD-TD method," *10th Niigata Branch Regional Meeting of IEE Japan*, III-21, Nov. 2001 (in Japanese).

[13] Y. Tange, Y. Kanai, and Y. Saitoh, "Analysis and development of a radio frequency rectangular resonant cavity applicator with multiple antennas

for a hyperthermic treatment," *IEEE Trans. on Magn.,* vol. 41, no. 5, pp. 1880-1883, May 2005.
[14] D. Sullivan, "Three-dimensional computer simulation in deep regional hyperthermia using the finite-difference time-domain method," *IEEE Trans.* on *Microwave Theory Tech.*, vol. 38, no. 2, pp. 204-211, Feb. 1990.
[15] G. Badger, "New class of coaxial-line transformers," *ham radio*, pp. 18-29, Mar. 1980.
[16] Y. Tange, Y. Kanai, and Y. Saitoh, "Heating characteristics of an RF hyperthermia for deep-seated region," *Proc. Annual Int'l Conf. of the IEEE Eng. in Medicine and Biology Society*, 271, 2005.
[17] S. Hoshina, Y. Kanai, and M. Miyakawa, "A numerical study on the measurement region of an open-ended coaxial probe used for complex permittivity measurement," *IEEE Trans. on Magn*., vol. 37, no. 5, pp. 3311-3314, Sep. 2001.
[18] Federal Communications Commission web site [Online]. Available, (http://www.fcc.gov/fcc-bin/dielec.sh/).
[19] JSME, *JSME Data Book, Heat transfer*, 4th ed., Tokyo: JSME Press, p. 321, 1986 (in Japanese).
[20] A. R. von Hippel, *Dielectric Material and Applications*, 3rd ed., Boston: The M.I.T. Press, p. 359, 1961.
[21] K. R. Umashankar, A. Taflove, and B. Beker, "Calculation and experimental validation of induced currents on coupled wires in an arbitrary shaped cavity," *IEEE Trans. on Antennas Propagat*., vol. 35, no. 11, pp. 1248-1257, Nov. 1987.
[22] Y. Kanai and K. Sato, "Automatic mesh generation for 3D electromagnetic field analysis by FD-TD method," *IEEE Trans. on Magn*., vol. 34, no. 5, pp. 3383-3386, Sep. 1998.
[23] T. Uno, *Finite difference time domain method for electromagnetic field and antennas*, Tokyo: Corona Publishing, 2000, pp. 50-55 (in Japanese).

Yutaka Tange received his B. E. and M. E. degrees in mechanical engineering from Toyohashi University of Technology in 2001 and 2003. From 2003, he has been a Ph.D. candidate at Niigata University. His research theme is the development of hyperthermia systems for deep-seated tumor. He is a member of Japanese Society of Hyperthermic Oncology (JSHO), IEICE and Journal of the Japan Society of Mechanical Engineers (JASME).

Yasushi Kanai was born in Niigata, Japan in 1959. He received the B. E., M. E. and Dr. Eng. degrees from Niigata University in 1982, 1984 and 1989, respectively. In 1984, he joined Alps Electric, Co., Ltd., Japan and worked as a research engineer until 1992. From 1992 to 1995, he was with Niigata University as an Associate Professor. In 1995, he joined Niigata Institute of Technology. Since 1999, he has been a Professor at the Department of Information and Electronics Engineering, Niigata Institute of Technology. His main research interests are numerical computations of electromagnetic fields and magnetic recording. He received The Valued Service Award from ACES in March 2003. Prof. Kanai is an ACES Journal Associate Editor, a Member of IEEE and a Founder Member of International Compumag Society.

Yoshiaki Saitoh received his B.E. degree in electrical engineering from Niigata University in 1963, and M.E. and Ph.D. degrees in electrical engineering from Hokkaido University in 1965 and 1970. In 1965, he joined the staff of the Department of Electronics, Niigata University, as an instructor, and had been a professor in the Department of Information Engineering since 1980. He is currently a professor in the Department of Biocybernetics. His recent research interests include measurements and stimulation of human organs, hyperthermia systems, and biomedical signal processing. He is a Senior Member of IEEE and the Japan Society of Medical Electronics and Biological Engineering.

Tatsuya Kashiwa graduated from the Department of Electrical Engineering of Hokkaido University in 1984 and completed the M.S. program in 1986. Before completing the doctoral program, he became a research associate in Department of Electrical Engineering in 1988. He has been an associate professor in the Department of Electrical and Electronic Engineering of Kitami Institute Technology since 1996. His research area is the analysis of electromagnetic fields and acoustic fields. He received an IEEE AP-S Tokyo Chapter Young Engineer Award in 1992. He is a coauthor of *Handbook of Microwave Technology* (Academic Press) and *Antenna and Associated System for Mobile Satellite Communications* (Research Signpost). He is a reviewer for IEEE MTT. He holds a Dr. Eng. degree, and is a member of IEICE and IEEE.